ROYAL SOCIETY
OF CHEMISTRY

PAPER

Monitoring guanine photo-oxidation by enantiomerically resolved Ru(II) dipyridophenazine complexes using inosine-substituted oligonucleotides

Páraic M. Keane,*[ab] Fergus E. Poynton,[ac] James P. Hall,[bd] Ian P. Clark,[e] Igor V. Sazanovich,[e] Michael Towrie,[e] Thorfinnur Gunnlaugsson,[ac] Susan J. Quinn,[f] Christine J. Cardin*[b] and John M. Kelly*[a]

The intercalating $[Ru(TAP)_2(dppz)]^{2+}$ complex can photo-oxidise guanine in DNA, although in mixed-sequence DNA it can be difficult to understand the precise mechanism due to uncertainties in where and how the complex is bound. Replacement of guanine with the less oxidisable inosine (I) base can be used to understand the mechanism of electron transfer (ET). Here the ET has been compared for both Λ- and Δ-enantiomers of $[Ru(TAP)_2(dppz)]^{2+}$ in a set of sequences where guanines in the readily oxidisable GG step in ${TCGGCGCCGA}_2$ have been replaced with I. The ET has been monitored using picosecond and nanosecond transient absorption and picosecond time-resolved IR spectroscopy. In both cases inosine replacement leads to a diminished yield, but the trends are strikingly different for Λ- and Δ-complexes.

Introduction

The non-covalent binding of metal complexes to double-stranded DNA is a challenging example of supramolecular chemistry. As has been amply shown over the years it is not always straightforward to determine precisely how the molecule binds to the duplex (intercalation, semi-intercalation, binding in the minor- or major-grooves, or simple external binding).[1] A further interesting aspect for octahedral complexes with bidentate ligands is the fact that two enantiomers exist, opening up the possibility of stereo-specific binding.[2] As many of these

[a]School of Chemistry, Trinity College, Dublin 2, Ireland. E-mail: keanepa@tcd.ie; jmkelly@tcd.ie

[b]Dept. of Chemistry, University of Reading, Whiteknights, Reading, RG6 6AD, UK. E-mail: c.j.cardin@rdg.ac.uk

[c]Trinity Biomedical Sciences Institute, Dublin 2, Ireland

[d]Diamond Light Source, Harwell Science and Innovation Campus, Oxfordshire, OX11 0QX, UK

[e]Central Laser Facility, Research Complex at Harwell, STFC Rutherford Appleton Laboratory, Harwell Science and Innovation Campus, Oxfordshire, OX11 0QX, UK

[f]School of Chemistry, University College Dublin, Dublin 4, Ireland

complexes can act as photosensitisers of DNA damage, it is vital that one knows as much as possible about the location, mode of binding and precise orientation of the molecule relative to the target part of the nucleic acid. In this connection crystallography studies can be of great use.[3] However, given the sensitivity of binding to the surrounding medium and to concentrations of the constituents, it is possible that the precise non-covalent interaction of the metal complex with the polynucleotide in solution may be different. (For example semi-intercalation may be favoured in the crystal). In this paper we extend our studies of factors determining photo-induced one-electron oxidation of DNA by $[Ru(TAP)_2(dppz)]^{2+}$ (**1**, Fig. 1; TAP = 1,4,5,8-tetraaza-phenanthrene; dppz = dipyrido[3,2-a:2′,3′-c]phenazine) using ultrafast transient spectroscopy, by examining the effect of replacing the readily oxidisable guanine by inosine. As we will show, this substitution can have surprising effects which are due to the supramolecular association of the metal complex enantiomer with the duplex DNA. Developing our understanding of the mechanism for such photo-sensitised DNA damage is also important for phototherapeutic applications.[4]

Dipyridophenazine complexes of ruthenium, such as $[Ru(phen)_2(dppz)]^{2+}$ (phen = 1,10-phenanthroline) or $[Ru(TAP)_2(dppz)]^{2+}$ bind strongly to DNA by intercalation of the dppz ligands between the DNA base-pairs.[5] Although structurally similar, the phen and TAP derivatives have markedly different photophysical properties, and it has been shown that racemic **1** photo-oxidises guanine in either polynucleotide DNA or in mononucleotide GMP,[6] which results in luminescence quenching. The reduced metal complex and oxidised guanine species can then be observed using picosecond transient visible absorption and time-resolved IR, respectively. Other TAP complexes have been shown to form a covalent photo-adduct with guanine upon photolysis.[7] The proposed mechanism for ET is shown in Scheme 1, although it is not at this stage clear whether the process proceeds by direct or proton-coupled ET.
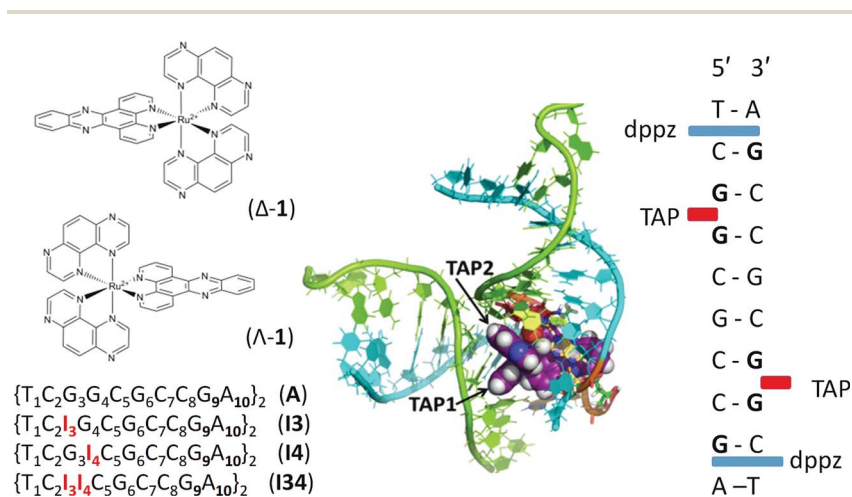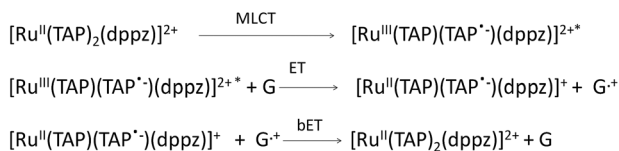

Fig. 1 Structures of Λ- and Δ-$[Ru(TAP)_2(dppz)]^{2+}$; ODNs **A**, **I3**, **I4** and **I34**; crystal structure of Λ-$[Ru(TAP)_2(dppz)]^{2+}$ in ODN **A** (adapted from Hall *et al.*[3a]); intercalation and semi-intercalation sites in crystal structure.

$$[Ru^{II}(TAP)_2(dppz)]^{2+} \xrightarrow{MLCT} [Ru^{III}(TAP)(TAP^{\bullet-})(dppz)]^{2+*}$$

$$[Ru^{III}(TAP)(TAP^{\bullet-})(dppz)]^{2+*} + G \xrightarrow{ET} [Ru^{II}(TAP)(TAP^{\bullet-})(dppz)]^{+} + G^{\bullet+}$$

$$[Ru^{II}(TAP)(TAP^{\bullet-})(dppz)]^{+} + G^{\bullet+} \xrightarrow{bET} [Ru^{II}(TAP)_2(dppz)]^{2+} + G$$

Scheme 1   A mechanism for the photo-oxidation of G by $[Ru(TAP)_2(dppz)]^{2+}$.

We recently compared the resolved $\Lambda-$ and $\Delta-$ enantiomers for the first time to show that the enantiomeric conformation and DNA sequence can modulate the electron transfer considerably.[6e] We have since shown that efficient formation of the reduced species requires the complex to be bound at a G-containing site while ET over a longer distance results in a significant reduction in yield and rate.[6f] Accurate understanding of the photo-oxidation requires knowledge of where and how the complex is bound. This problem has been helped greatly since the precise geometry of the binding site for such $[Ru(\text{II})(dppz)]^{2+}$ complexes has been defined recently from X-ray crystallography.[3] The first such structure reported for a DNA-bound Ru(II)dppz complex was for Λ-**1** in the presence of the $\{TCGGCGCCGA\}_2$ decamer duplex.[3a] The crystal structure of Λ-**1** bound to $\{TCGGCGCCGA\}_2$ shows intercalation at the terminal T1C2; G9A10 step, and semi-intercalation of the TAP ligand at the G3G4 step (Fig. 1). The $\{TCGGCGCCGA\}_2$ duplex is also notable for containing a GG step, a well-known damage hotspot due to the lowered oxidation potential of the 5′-G.[8]

In our recent study on the enantiomers of **1** we suggested that binding of the $\Lambda-$ complex close to GG sites may be the cause of increased yields of ET. Therefore, in this current study, we have substituted G3 and G4 in $\{TCGGCGCCGA\}_2$ with inosine in order to observe the effect on the ET. Inosine is structurally similar to guanine, but with the NH_2 at the 2 position removed, and is reported to have an oxidation potential 200 mV higher than guanine.[9] It still forms a base-pair with C, and can be substituted into a DNA sequence. It is not expected to perturb the structure of the DNA,[10] although a slight bending[11] and decrease in melting temperature may be found due to the removal of one Watson–Crick hydrogen bond. The strategy of inosine substitution has been used previously in order to assign sites of damage and learn information on the ET mechanism.[12] However, our previous crystallographic data has revealed that, in some circumstances, and in particular for the $\Lambda-$ enantiomer, slight changes in sequence can have a large effect on the binding modes.[3b] As replacing G with I means the removal of one NH_2 group, the CI base-pair has been noted to be sterically and electronically similar to a TA base-pair when viewed from the minor groove, the site from which these complexes approach (Fig. 2).[13] Therefore, it is intriguing to observe the effect of inosine substitution on the ET for each enantiomer.

To study the photo-sensitised oxidation process we have used ultrafast time-resolved spectroscopy. Transient absorption (TrA) is used to monitor the visible region spectroscopic changes at the polypyridyl complex, while time-resolved infrared (TRIR) is especially useful for following chemical changes in the nucleobases.[14] D_2O is used as the solvent due to strong absorptions by H_2O in the 1650 cm^{-1} region. Typical concentrations of 400 μM $[Ru(\text{II})(TAP)_2(dppz)]^{2+}$ and 500 μM
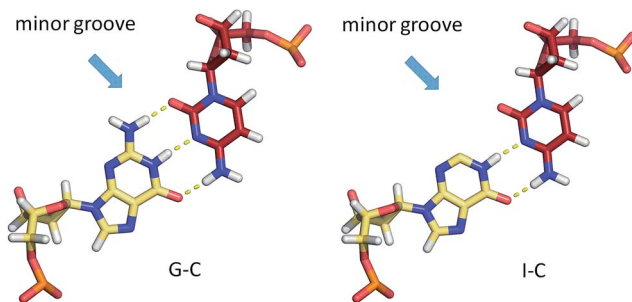
Fig. 2 Comparison of the G-C and I-C base pairs with respect to the minor groove.

DNA duplex were used to allow TrA and TRIR to be performed on comparable samples. Statistically under these conditions only one complex is bound per duplex.

Experimental

The Λ/Δ-[Ru(TAP)$_2$(dppz)]$^{2+}$ complex was synthesised and resolved using modified literature methods.[6e] Time-resolved measurements were performed on the ULTRA apparatus at the Central Laser Facility (Harwell, UK), described in detail elsewhere.[15a] Briefly, the spectrometer comprises a 10 kHz repetition rate titanium:sapphire amplifier producing 0.8 mJ output with 40 fs pulse duration, at 800 nm. Optical parametric amplifiers and second harmonic generation of the 800 nm output created the mid-infrared radiation and 400 nm femtosecond pump pulses for psTRIR measurements. For the ps-TrA measurements, part of the titanium:sapphire laser output beam was used to generate a white light continuum in a CaF$_2$ crystal. The polarisation of the pump pulses at the sample was at the magic angle relative to the probe. For nanosecond experiments excitation was at 355 nm and pulse length was 1 ns. The excitation pulse energy at the sample was *ca.* 0.8–1 μJ and focused to approximately 100 μm spot size. Ns-TrA spectra for Λ/Δ-**1** bound to ODNs **I3** and **I4** were recorded using the time-resolved multiple probe spectroscopy (TR^{M}PS) configuration at 400 nm excitation.[15b] The set-ups for psTrA/TRIR and nsTrA are identical to those described in detail recently.[6e,f] Data analysis was performed using OriginPro 8.5. Single exponential growth kinetics were calculated at single wavelengths using the Marquardt–Levenburg algorithm.

Results

The visible transient absorption (TrA) difference spectrum observed shortly after 400 nm laser pulse excitation of [Ru(TAP)$_2$(dppz)]$^{2+}$ in aqueous buffer (pH 7) solution shows strong bleaching between approximately 420 nm and 500 nm and broad absorption at longer wavelengths with a maximum at *ca.* 600 nm (Fig. 3 & 4).[6e] Very similar spectra are found at times shortly after the laser pulse when the complex is bound to any of the oligodeoxynucleotides (ODN) used in this study (Fig. 3 shows spectra recorded 20 ps after laser excitation). This species may be assigned as the [Ru(III)(TAP)(TAP$^{•-}$) (dppz)]$^{2+*}$ ^{3}MLCT excited state localised on
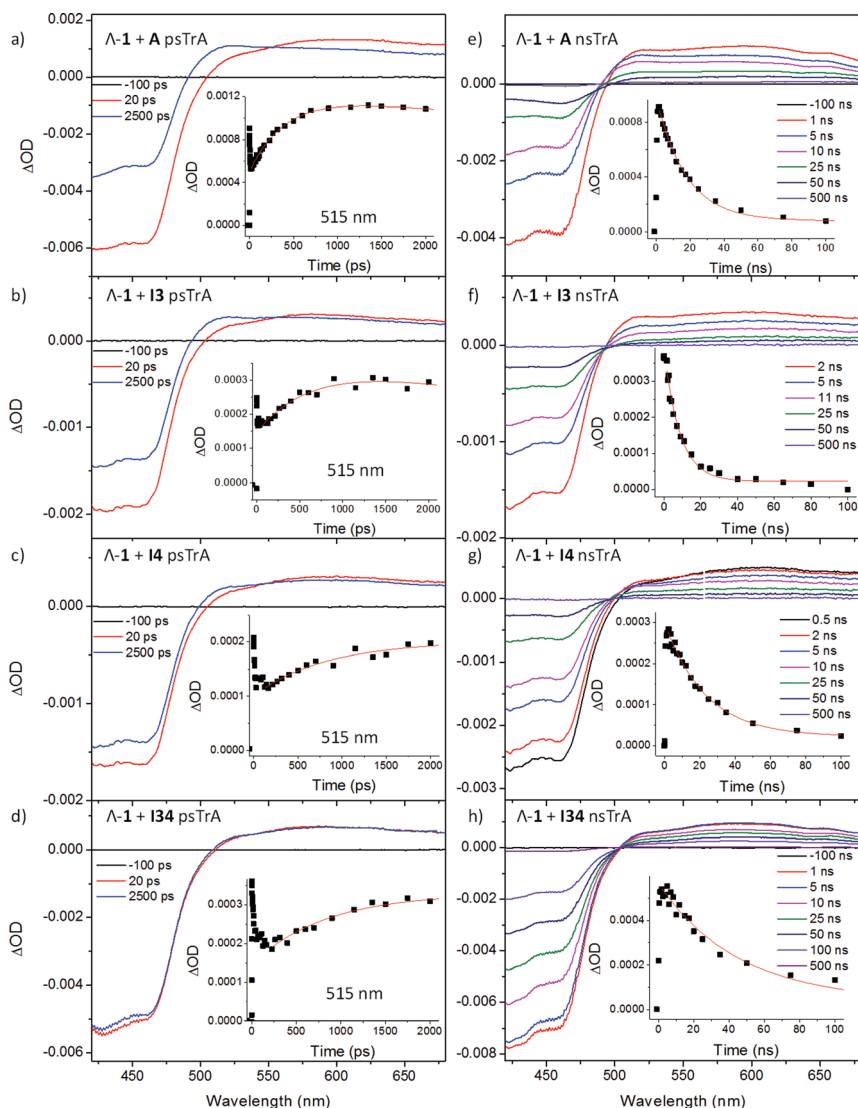
Fig. 3 Comparison of ps/ns-TrA spectra of Λ-[Ru(TAP)$_2$(dppz)]$^{2+}$ in the presence of **A**, **I3**, **I4** or **I34**; λ_{exc} = 400 nm (a–d, f and g); 355 nm (e and h) at 1 μJ. Inset: kinetics at 515 nm (note the differences in strength of signal in ps-TrA data). Data in the presence of **A**[6e] shown for comparative purposes (panel (a) adapted, with permission, from Keane et al.[6e]).

the TAP ligand.[6] At later times a new feature emerges with an absorption maximum at 515 nm, which is assigned to [Ru(II)(TAP)(TAP$^{\bullet-}$)(dppz)]$^+$, formed by reduction of the complex's excited state through electron transfer from guanine. The extent to which this feature develops (which can be monitored by measuring the ΔOD (515 nm) : ΔOD (600 nm) ratio) is very sensitive to the ODN to which the complex is bound.[6e] It may also be noted that the intensity of the negative-going band in the 420–500 nm region also diminishes strongly as the electron transfer reaction proceeds. This diminution of the bleach band is due to the reduced
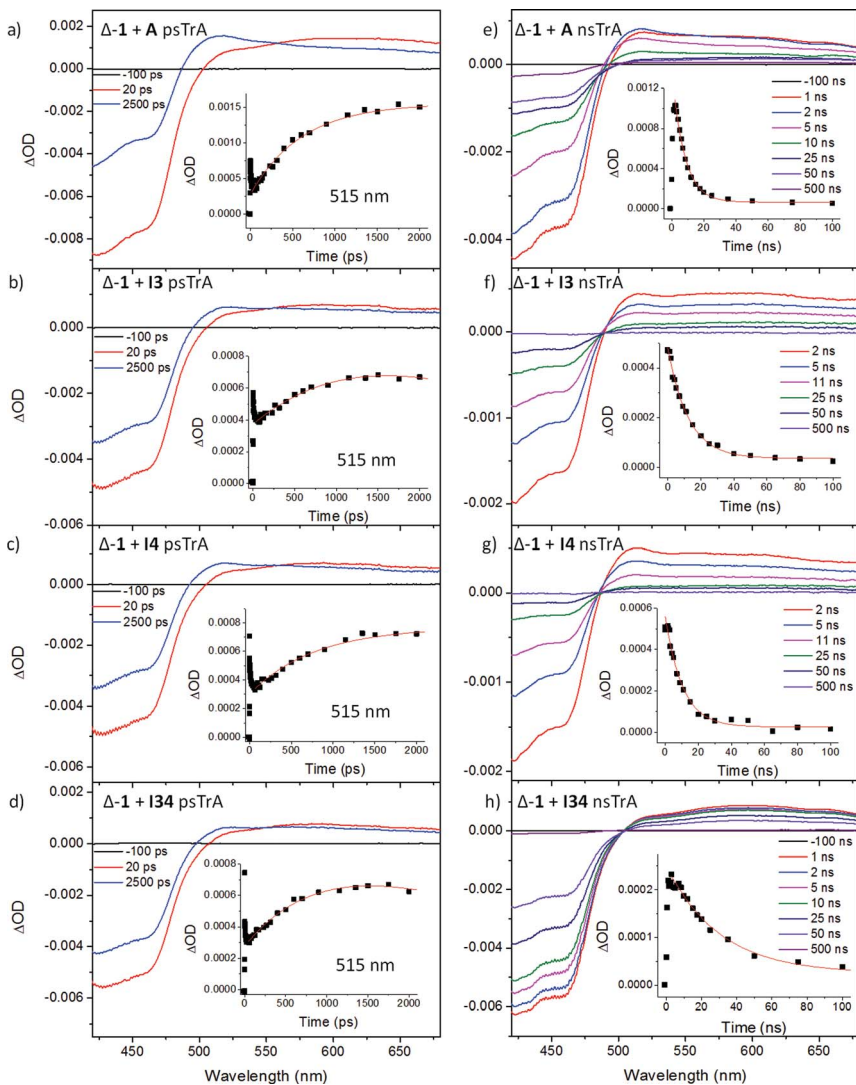
Fig. 4 Comparison of ps/ns-TrA spectra of Δ-$[Ru(TAP)_2(dppz)]^{2+}$ in the presence of A, I3,I4 or I34. λ_{exc} = 400 nm (a–d, f and g); 355 nm (e and h) at 1 µJ. Inset: kinetics at 515 nm (note the differences in strength of signal in the ps data). Data in the presence of A[6e] shown for comparative purposes (panel (a) adapted, with permission, from Keane et al.[6e]).

Table 1 Relative ET yields determined from bleach intensities[a]

Complex	A[b]	I3	I4	I34	(GC)$_5$[b]	G$_5$C$_5$[b]
Λ	0.44	0.28	0.14[c]	0.05[c]	0.22	0.74
Δ	0.57	0.32	0.35	0.25	0.62	0.64

[a] Calculated as $(\Delta OD_{20\,ps} - \Delta OD_{2500\,ps})/\Delta OD_{20\,ps}$ at 460 nm. [b] Values calculated from data in Keane et al.[6e] [c] As in this case ΔOD has not reached its lowest value at 20 ps, the ET ratio has been calculated using $\Delta OD_{100\,ps}$ in place of $\Delta OD_{20\,ps}$ in the above equation.

species absorbing more strongly than the excited state. This change (measured using the absorbance ratio at 20 ps and at 2500 ps) can therefore be used as a means to measure the relative yield of electron transfer (see Fig. 3 & 4 and Table 1, data for $\{(GC)_5\}_2$ and $\{G_5C_5\}_2$ have also been included for comparative purposes).† This data shows that for Λ-**1** the relative yield decreases very strongly in the order **A** > **I3** > **I4** > **I34**. By contrast for Δ-**1**, the yields of electron transfer with **I3**, **I4** and **I34** are quite similar and approximately half that found with **A**.

Kinetics of the rate of forward ET can be readily measured by monitoring the increase in absorption at 515 nm. It may be observed that for Λ-**1** the rate is somewhat slower for **I4** than it is for **A** and **I3**, while for Δ-**1** the rate for **I3** is faster than for **A** and **I4** (Table 2).

The transient absorption and bleaching signals decay in the nanosecond time domain, showing that the system is reversible. In all cases this decay is more than an order of magnitude faster than the excited state free in solution or when bound to a guanine-deficient duplex such as poly$\{dA–dT\}_2$.[6b] Such rapid decay is found to occur at both 515 nm and at 600 nm and first order rate constants measured for **A**, **I3**, or **I4** at these wavelengths are the same within error. For Λ-**1** the rates decrease in the order **I3** > **A** > **I4**, while for Δ-**1** the order is **A** > **I3**, **I4**. For both enantiomers the **I34** system has a lifetime of ca. 45 ns.

In contrast with TrA experiments, TRIR allows the monitoring of spectroscopic changes on the ODNs as well as on the metal complex. The latter dominate the spectra below 1500 cm^{-1} with many sharp bleaches and transients, including a

Table 2   Fitted lifetimes for TrA and TRIR spectra of Λ- and Δ-[Ru(TAP)$_2$(dppz)]$^{2+}$ bound to A, I3, I4 or I34

Wavelength/ wavenumber	A^a	I3	I4	I34
Λ				
Ps-TrA (515 nm)	410 ± 40 ps	650 ± 80 ps	820 ± 100 ps	820 ± 190 ps
Ns-TrA (515 nm)	17 ± 3 ns	11 ± 2 ns	28 ± 3 ns	45 ± 5 ns
Ps-TRIR (1680 cm^{-1})	460 ± 90 ps	790 ± 160 ps	780 ± 160 ps	Nd^b
Δ				
Ps-TrA (515 nm)	730 ± 70 ps	520 ± 50 ps	790 ± 80 ps	590 ± 60 ps
NsTrA (515 nm)	8 ± 1 ns	13 ± 2 ns	11 ± 2 ns	40 ± 5 ns
Ps-TRIR (1680 cm^{-1})	860 ± 170 ps	740 ± 150 ps	1180 ± 240 ps	Nd^b

^{a} Data from Keane et al.[6e] ^{b} Nd = not determined due to weak signal.

† If it is assumed that at 20 ps after the laser pulse the only transient species present is the excited state having an absorption coefficient ε_{es}, then the change in absorbance (ΔOD_{20ps}) will be proportional to (ε_{es} − ε_{gs}), where ε_{gs} is the absorption coefficient of the ground state at the same wavelength. If the excited state were to be converted 100% to the reduced complex, then ΔOD after reaction will be proportional to (ε_{red} − ε_{gs}), where ε_{red} is the absorption coefficient of [Ru(TAP)$_2$(dppz)]$^+$. If only a fraction (x) of the excited states is so converted, then ΔOD is proportional to $x(\varepsilon_{red}$ − $\varepsilon_{gs}) + (1 − x) (\varepsilon_{es}$ − $\varepsilon_{gs})$. If we assume that at 2500 ps any reaction of the excited state on the picosecond timescale is complete and that the only process excited states have undergone is reduction giving [Ru(TAP)$_2$(dppz)]$^+$, then ($\Delta OD_{2500\ ps}$ − $\Delta OD_{20\ ps})/\Delta OD_{20\ ps} = x(\varepsilon_{red}$ − $\varepsilon_{es})/(\varepsilon_{es}$ − $\varepsilon_{gs})$, so that comparing this parameter with various ODNs gives a measure of the relative yield of electron transfer.

large broad absorption at 1460 cm^{-1} found in both the MLCT excited state and the reduced complex (Fig. 5).[6e] Strong bleaching is also observed between 1640 cm^{-1} and 1700 cm^{-1}, where the C=O absorptions of C and G or I occur. (Fig. 2). As the DNA is not directly excited at 400 nm, these bleaches can be attributed to changes in the structure of the G-C or I-C base pairs upon photo-excitation of the bound complex. The presence of these bands at early times (∼20 ps) before ET has occurred must be due to an interaction between the photo-excited metal complex and the nucleobases in the binding site. As previously reported[6e] the subsequent
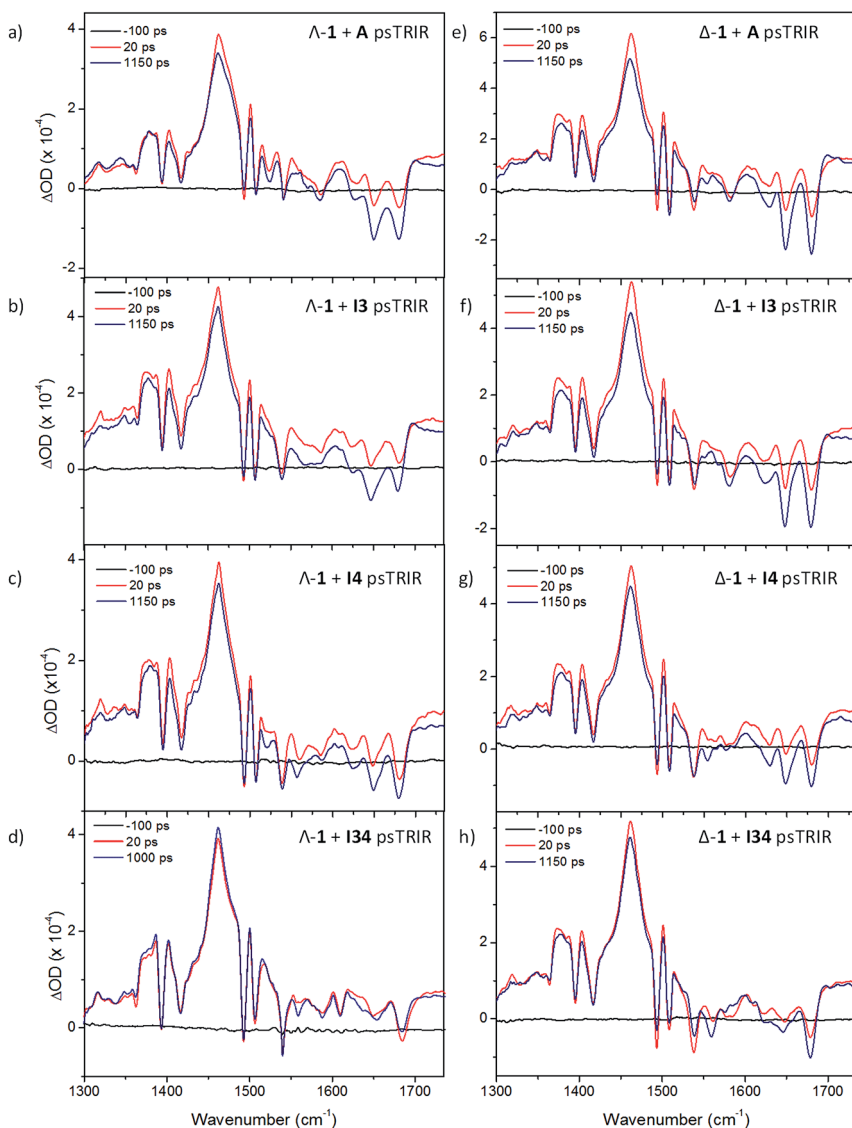

Fig. 5   Comparison of ps-TRIR spectra of Λ and Δ-[Ru(TAP)$_2$(dppz)]$^{2+}$ in the presence of **A**, **I3**, **I4** or **I34**. λ_{exc} = 400 nm. Data in the presence of **A**[6e] shown for comparative purposes.

electron transfer process leads to a characteristic increase in the bleaching of these carbonyl bands (G, 1680 cm^{-1}) with first order rate constants consistent with those determined for the formation of the reduced ruthenium complex by TrA. Concurrently an absorption band at approximately 1700 cm^{-1} appears, which is assigned to the one-electron oxidised guanine.[16] Such features are found for **A** and for **I3** ODNs with both enantiomers. The situation is less clear for **I4** and **I34**. As expected from the TrA studies, the reduced ET yield with **I4** is consistent with the modest additional bleaching between 20 and 1000 ps for the Λ− enantiomer. For the **I34** samples there is increased bleaching for the Δ− enantiomer, although the band at 1700 cm^{-1} is not well developed. It may be noted that in this case the bleaching pattern does differ significantly from that of the other oligonucleotides, perhaps indicative of a different binding site.

Discussion

The above experiments show that substituting G3/G4 by inosine in the self-complementary duplex sequence {TCGGCGCCGA}$_2$ has a major effect on both the yield of electron transfer to photo-excited intercalated **1** and on the rates of the subsequent back electron transfer. Given that the oxidation potential for inosine is reported to be *ca.* 200 mV less favourable than guanine[9] it is unsurprising that the yield of electron transfer (with resultant production of the reduced photo-sensitiser) is sensitive to this substitution. This effect is expected to be particularly large at G3G4 as GG sites are known to be 'hotspots' for photo-oxidation.[8] Our data also shows that the one-electron photo-oxidation depends markedly on the enantiomer employed. This we believe is largely determined by the supramolecular forces controlling the non-covalent binding of the metal complex to the DNA. In particular, given that it appears that the electron transfer from guanine to the photoexcited state of [Ru(TAP)$_2$(dppz)]$^{2+}$ only occurs when the complex is in contact with a guanine-containing base-pair,[6f] it is likely that any preference for particular base-pair steps will be crucial.

Initially, it is worth considering whether the inosine substitution would have an effect on the secondary structure of the native DNA. Melting studies have shown that G/I substitution causes structural changes extending up to 5 base-pairs away, and which are sequence dependent.[17] Molecular dynamics simulations comparing {CGCGAATTCGCG}$_2$ and {CGCIAATTCGCG}$_2$ reveal an increased intrinsic flexibility of the latter (although no change in curvature relative to the native ODN) possibly due to changes in the hydration of the groove and destacking of the bases.[18] By contrast, gel mobility experiments suggest that increased curvature may be seen in I-substituted ODNs,[11] although the X-ray structure of {CGCIAATTCGCG}$_2$ shows an isomorphous structure to {CGCGAATTCGCG}$_2$, with similar structures for both GC and IC sites.[10] However, it is likely that the presence of the intercalator would provide significant stabilisation to the duplex, and differences in binding preference would be more likely to be caused by removal of NH$_2$ from the intercalation site, than on the secondary structure of the duplex.

In discussing preferences for particular base-steps it is interesting to consider the insights which may be provided by the crystal structures of [Ru(II)L$_2$(dppz)]$^{2+}$ complexes bound to oligonucleotides.[3] Such structures have been reported mainly for the Λ-isomer, so our discussion will focus initially on that enantiomer.

It may also be noted that the base-pair steps may be classified as symmetric or asymmetric – the former leading to a perpendicular insertion of the intercalating dppz, while the latter will lead to a canted (or angled) orientation (Fig. 6).

In considering the symmetric mode for binding of Λ-**1** to oligonucleotides it is clear that binding to a TA,TA base step may be preferred. This is apparent from our study on {CCGGTACCGG}$_2$ and {CCGGATCCGG}$_2$ where it was found that intercalation occurred at the central TA,TA base step, but not at AT,AT.[3b] This preference is also found with these ODNs in solution and has been shown to have a controlling influence on the yield of electron transfer.[6f] Additionally no inter-calated complex is found at the central CG,CG step in the crystal structure of Λ-**1** bound to oligonucleotide **A**,[3a] which may be taken as an indication that this site is also less favoured than that of TA,TA and which can be correlated with hindrance of binding by the exocyclic amino-group of the guanine (Fig. 6). The above results suggest that for these symmetrical sites the order of preference of binding should be in the order TA,TA > CG,CG > AT,AT or GC,GC.

In all the crystal structures we have determined for this family of oligonucle-otides, the complex intercalates at the terminal pyr·pyr,pur·pur base step, inserting with a canted orientation.[3a,b] This suggests that this may also be a favourable binding site in solution, although it should be noted that in the crystal structures, semi-intercalation of a TAP ligand at the G3G4,C7C8 step blocks
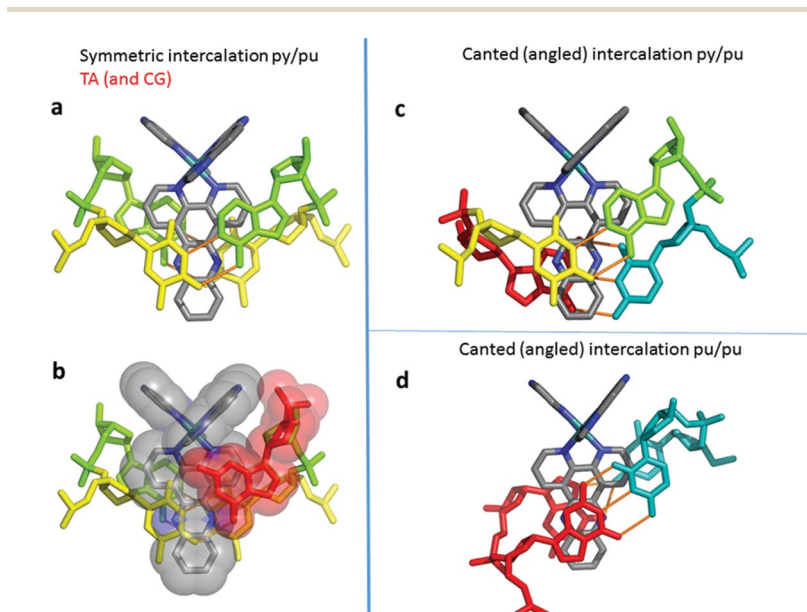

Fig. 6 Binding modes of the Λ-enantiomer determined by X-ray crystallography for {CCGGTACCGG}$_2$.[3b] (a) Symmetrical intercalation from the minor groove at a TA/TA step[3b] (b) superimposition of space-filling model of a guanine residue on (a) to show the steric clash with the 2-NH$_2$ of the guanine base. (c) An asymmetric pyrimidine–purine step with asymmetric (angled) intercalation from the minor groove. The CA/TG step.[3e] (d) fully angled (canted) intercalation at a purine–purine step. The terminal GG/CC step (with Hoogsteen and Watson–Crick base pairs.[3b] Colour code for residues: G – red, A – green, C – cyan, T – yellow. The ruthenium complex is grey, with nitrogen – blue and ruthenium – teal.

intercalation at and near this part of the duplex and so may give a distorted picture of binding preference. (By contrast, semi-intercalation is expected to be only a minor component in solution due to a relatively low binding constant.[19]) The crystal structure shows that a further important factor in the binding at pur·pur,pyr·pyr base step sites is the overlap of the dppz with the purine. We have also found that both enantiomers of [Ru(phen)$_2$(dppz)]$^{2+}$ bind at the TG,CA step of d(ATGCAT)$_2$,[3c] suggesting that this pyr·pur,pyr·pur base pair step is also a favoured site, as has previously been shown for some classic intercalators.[1]

Turning to consider the inosine-substituted duplexes, it may be noted that the I–C base-pair is electronically and sterically more similar to an AT base-pair than a GC one, when viewed from the minor groove (Fig. 2), the site of intercalation for [Ru(II)L$_2$(dppz)]$^{2+}$ complexes. It is therefore probable that the distribution of binding sites may be quite different in **A**, **I3**, **I4** and **I34**, as it might be expected that a CI,CG base pair step would be a stronger binding site compared to a CG,CG one (see Fig. 6a and b). As noted above, this might have an effect on the yield of ET, as it is normally assumed that binding close to contiguous G (such as G3G4) gives a high yield. In the case of ODN **A**, this would mean binding at the C2G3,C8G9 or at the G4C5,G6C7. From the considerations given above the former should be one of the preferred sites for that duplex, while substitution by I of G3 or G4 would generate the new base-pair steps C2I3,C8G9 or I4C5,G6C7. The former might be considered a favoured one as it could be considered to be similar to a CA,TG site, which would therefore increase the population at that site. On the other hand changing G4C5,G6C7 for I4C5,G6C7 would probably have only a minor effect on the preferred binding site.

Perhaps the most dramatic effect for the Λ-complex is when both G3 and G4 are substituted, where the ET appears to be completely eliminated. This might indicate that the complex intercalates at this I3I4,C7C8 site where, of course, it is not in contact with any guanine. As remarked upon earlier, previous studies with [Ru(TAP)$_2$(dppz)]$^{2+}$ have suggested that contact of the complex with guanine is necessary for efficient ET. It is also notable that the yield of ET is much more strongly suppressed compared to the unsubstituted **A** when G4 is replaced with inosine than is the case for **I3**. This behaviour may be contrasted with that reported by Sistare *et al.* for the oxidation of oligonucleotides by electrochemically-generated [Ru(bpy)$_3$]$^{3+}$.[12c] They reported that the ratio of oxidation rate constants for 5′-GI and 5′-IG steps is $k_{GI}/k_{IG} = 2.8$. Much of the difference between our study and that of Sistare *et al.* may be attributed to the differing non-covalent binding properties of [Ru(bpy)$_3$]$^{2+}$ and [Ru(TAP)$_2$(dppz)]$^{2+}$. Thus [Ru(bpy)$_3$]$^{2+}$ associates weakly to duplex DNA, probably in the grooves, with relatively little sequence specificity.[19] By contrast [Ru(TAP)$_2$(dppz)]$^{2+}$ (like its structural analog [Ru(phen)$_2$(dppz)]$^{2+}$) intercalates into the duplex. It is also noteworthy that intercalation into the GG step is likely to perturb the GG stacking that is crucial for lowering the oxidation potential.[8]

Turning to the behaviour of the Δ-enantiomer, it may be noted that in a previous study comparing Λ-**1** and Δ-**1** in ODN **A**, {(GC)$_5$}$_2$ and {G$_5$C$_5$}$_2$, we showed that for Δ-**1** the rates and yield of ET in each sequence varied much less than those for Λ-**1**. Similarly in the current work it is found that the large variations observed for the Λ-enantiomer are not observed for the Δ-isomer. For example the yield of ET with **I34** is about 50% of that of ODN **A**, whereas it is tiny for Λ-**1**. Additionally it may be noted that the yields of ET with Δ-**1** are similar for **I3**, **I4**, or **I34**, in

complete contrast with what is observed for its Λ-enantiomer. This may imply, as was postulated in our previous study,[6e] that the GG stack is not as important for Δ-**1** as for Λ-**1**, suggesting that Δ-**1** does not bind at this site. Indeed, the removal of both Gs at G3G4 does not reduce the yield to a similar extent compared to Λ-**1**, which suggests that high yields of ET can be found for Δ-**1** when the sequence contains only single Gs (as previously shown with {(GC)$_5$}$_2$).[6e] This is another example of how the enantiomers need to be regarded as distinct species in the context of their DNA-binding behaviour.

A notable feature of the TRIR is the presence of DNA bleaches on the ps timescale, before ET occurs. This is most likely due to the association of the excited-state complex with the nucleobases in the intercalation site. Notably, DNA features are also seen when Λ-**1** is bound to poly{dA–dT}$_2$,[6f] implying that they do not only arise in cases where photo-oxidation is occurring. Such diagnostic features have also been reported in DNA-bound Re complexes,[20] and may therefore represent a method for assigning the binding site in solution, which can be difficult to achieve using conventional techniques. The TRIR spectra for either Λ-**1** or Δ-**1** bound to **I34** both show a relatively larger bleach in the G/I region compared to that for C. It may be noted that, in an I-C base pair, the C carbonyl does not form a Watson–Crick H bond, and that the bleach profile shows some resemblance to the IR spectrum of inosine-rich DNAs such as poly{dI–dC}$_2$.[21] The physical basis for this interaction is unclear and merits further investigation, although it may be noted that photo-excitation results in a reduced metal centre, which may interact differently with the base pairs than does the ground state.

As shown in Table 2 there is no clear trend for the dependence of the rates of the forward and back reactions on the inosine substituent. The forward ET proceeds by transfer of an electron to the Ru(III) metal centre of the MLCT excited state. By contrast, the reverse ET involves transfer of an electron from the reduced TAP ligand and as a result, the geometric factors influencing the forward and back ETs in [Ru(TAP)$_2$(dppz)]$^{2+}$ are likely to be different. For the forward reaction the distance may be important, but it is also possible that overlap with the dppz ligand may be a significant factor. It has been proposed in computational studies on **1** that a $\pi\pi^*$ state on the dppz ligand may have an influence on the ET,[22] although most experimental evidence, including the TRIR spectra, points to the lowest excited state being of ML(TAP)CT type. The similarity of our TRIR spectra (in the region 1250–1500 cm^{-1}) when taken in solution or when the complex is bound to the ODNs strongly suggest that the same state is involved in both media.[6e] It is possible that overlap of dppz with the base-pairs contributes to the yield of ET, consistent with earlier reports that stressed the importance of the coupling between stacked units in photo-induced ET with classic intercalators such as thionine.[23] However it may be noted that the rate of forward ET observed with **1** ($\sim$1/500 ps) is slow compared to those photosensitisers. Also it would be misleading to state that the slower rate is purely due to geometric reasons, as the forward ET in the structurally similar [Cr(phen)$_2$(dppz)]$^{3+}$, which would be expected to bind similarly to DNA, occurs in less than 10 ps.[24] Whether the difference between the Cr(III) and the Ru(II) complexes is a consequence of energetics (the redox potential of the excited state of the Cr(III) is approximately 0.1 eV higher) or to a change in mechanism (from direct ET to proton-coupled) will require further investigation.

Concluding remarks

In conclusion this study shows that while replacing the guanosine nucleoside by inosine is not expected to affect the overall structure of the DNA duplex it can affect the nature of the binding sites, resulting in unexpected changes in the yield of electron transfer in certain cases. This is a further example of the sensitivity of small changes in DNA sequence, in this case the removal of a single NH_2 group in a decamer strand, on the binding mode of Ru(II)dppz complexes. Furthermore this highlights that the use of inosine substitution as a control experiment for guanine photo-oxidation should be performed with care, especially where the photosensitiser of interest binds from the minor groove. We are currently investigating the photophysics and crystal structures of $[Ru(TAP)_2(dppz)]^{2+}$ enantiomers bound to other ODNs, and it is anticipated that this will allow further insight into the relationship between DNA binding site and electron transfer dynamics for these complexes, and also into the binding modes and preferences that are common to both the crystal state and solution.

Acknowledgements

Notes and references

1 S. Neidle, *Nucleic Acid Structure and Recognition*, Oxford University Press, 2002.
2 (*a*) J. K. Barton, *Science*, 1986, **233**, 727–734; (*b*) C. Hiort, P. Lincoln and B. Nordén, *J. Am. Chem. Soc.*, 1993, **115**, 3448–3454.
3 (*a*) J. P. Hall, K. O'Sullivan, A. Naseer, J. A. Smith, J. M. Kelly and C. J. Cardin, *Proc. Natl. Acad. Sci. U. S. A.*, 2011, **108**, 17610–17614; (*b*) H. Niyazi, J. P. Hall, K. O'Sullivan, G. Winter, T. Sorensen, J. M. Kelly and C. J. Cardin, *Nat. Chem.*, 2012, **4**, 621–628; (*c*) J. P. Hall, H. Beer, K. Buchner, D. J. Cardin and C. J. Cardin, *Philos. Trans. R. Soc., A*, 2013, **371**, 20120525–20120532; (*d*) H. Song, J. T. Kaiser and J. K. Barton, *Nat. Chem.*, 2012, **4**, 615–620; (*e*) J. P. Hall, D. Cook, S. R. Morte, P. McIntyre, K. Buchner, H. Beer, D. J. Cardin, J. A. Brazier, G. Winter, J. M. Kelly and C. J. Cardin, *J. Am. Chem. Soc.*, 2013, **135**, 12652–12659; (*f*) J. P. Hall, H. Beer, K. Buchner, D. J. Cardin and C. J. Cardin, *Organometallics*, 2015, **34**, 2481–2486.
4 (*a*) N. A. Smith and P. J. Sadler, *Philos. Trans. R. Soc., A*, 2013, **371**, 20120519–20120532; (*b*) E. Wachter, D. K. Heidary, B. S. Howerton, S. Parkin and E. C. Glazer, *Chem. Commun.*, 2012, **48**, 9649–9651; (*c*) M. R. Gill and J. A. Thomas, *Chem. Soc. Rev.*, 2012, **41**, 3179–3192; (*d*) C. A. Puckett and J. K. Barton, *J. Am. Chem. Soc.*, 2007, **129**, 46–47; (*e*) R. B. P. Elmes, K. N. Orange, S. M. Cloonan, D. C. Williams and T. Gunnlaugsson, *J. Am. Chem. Soc.*, 2011, **133**, 15862–15865; (*f*) A. M. Palmer, S. J. Burya, J. C. Gallucci and C. Turro, *ChemMedChem*, 2014, **9**, 1260–1265; (*g*) L. Marcélis, C. Moucheron and A. Kirsch-De Mesmaeker, *Philos. Trans. R.*

Soc., A, 2013, **371**, 20120131; (*h*) S. M. Cloonan, R. B. P. Elmes, M. Erby, S. A. Bright, F. E. Poynton, D. E. Nolan, S. J. Quinn, T. Gunnlaugsson and D. C. Williams, *J. Med. Chem.*, 2015, **58**, 4494–4505.

5 (*a*) A. E. Friedman, J.-C. Chambron, J.-P. Sauvage, N. J. Turro and J. K. Barton, *J. Am. Chem. Soc.*, 1990, **112**, 4960–4962; (*b*) A. W. McKinley, P. Lincoln and E. M. Tuite, *Coord. Chem. Rev.*, 2011, **255**, 2676–2692; (*c*) A. Greguric, I. D. Greguric, T. W. Hambley, J. R. Aldrich-Wright and J. G. Collins, *J. Chem. Soc., Dalton Trans.*, 2002, 849–855.

6 (*a*) C. G. Coates, P. Callaghan, J. J. McGarvey, J. M. Kelly, L. Jacquet and A. Kirsch-De Mesmaeker, *J. Mol. Struct.*, 2001, **598**, 15–25; (*b*) I. Ortmans, B. Elias, J. M. Kelly, C. Moucheron and A. Kirsch-De Mesmaeker, *Dalton Trans.*, 2004, 668–676; (*c*) B. Elias, C. Creely, G. W. Doorley, M. M. Feeney, C. Moucheron, A. Kirsch-De Mesmaeker, J. Dyer, D. C. Grills, M. W. George, P. Matousek, A. W. Parker, M. Towrie and J. M. Kelly, *Chem.–Eur. J.*, 2008, **14**, 369–375; (*d*) J. A. Smith, M. W. George and J. M. Kelly, *Coord. Chem. Rev.*, 2011, **255**, 2666–2675; (*e*) P. M. Keane, F. E. Poynton, J. P. Hall, I. P. Clark, I. V. Sazanovich, M. Towrie, T. Gunnlaugsson, S. J. Quinn, C. J. Cardin and J. M. Kelly, *J. Phys. Chem. Lett.*, 2015, **6**, 734–738; (*f*) P. M. Keane, F. E. Poynton, J. P. Hall, I. V. Sazanovich, M. Towrie, T. Gunnlaugsson, S. J. Quinn, C. J. Cardin and J. M. Kelly, *Angew. Chem. Int. Ed.*, **54**, 8364–8368.

7 (*a*) J.-P. Lecomte, A. Kirsch-De Mesmaeker, M. M. Feeney and J. M. Kelly, *Inorg. Chem.*, 1995, **34**, 6481–6491; (*b*) L. Jacquet, R. J. H. Davies, A. Kirsch-De Mesmaeker and J. M. Kelly, *J. Am. Chem. Soc.*, 1997, **119**, 11763–11768.

8 I. Saito, T. Nakamura, K. Nakatani, Y. Yoshioka, K. Yamaguchi and H. Sugiyama, *J. Am. Chem. Soc.*, 1998, **120**, 12686–12687.

9 J. K. Barton, E. D. Olmon and P. A. Sontz, *Coord. Chem. Rev.*, 2011, **255**, 619–634.

10 J.-C. Xuan and I. T. Weber, *Nucleic Acids Res.*, 1992, **20**, 5457–5464.

11 C. Bailly, D. Suh, M. J. Waring and J. B. Chaires, *Biochemistry*, 1998, **37**, 1033–1045.

12 (*a*) S. O. Kelley and J. K. Barton, *Science*, 1999, **238**, 375–381; (*b*) C. Wan, T. Fiebig, O. Schiemann, J. K. Barton and A. H. Zewail, *Proc. Natl. Acad. Sci. U. S. A.*, 2000, **97**, 14052–14055; (*c*) M. F. Sistare, S. J. Codden, G. Heimlich and H. H. Thorp, *J. Am. Chem. Soc.*, 2000, **122**, 4742–4749; (*d*) F. Shao, M. A. O'Neill and J. K. Barton, *Proc. Natl. Acad. Sci. U. S. A.*, 2004, **101**, 17914–17919.

13 A. W. McKinley, J. Andersson, P. Lincoln and E. M. Tuite, *Chem.–Eur. J.*, 2012, **18**, 15142–15150.

14 M. Towrie, G. W. Doorley, M. W. George, A. W. Parker, S. J. Quinn and J. M. Kelly, *Analyst*, 2009, **134**, 1265–1273.

15 (*a*) G. M. Greetham, P. Burgos, Q. Cao, I. P. Clark, P. S. Codd, R. C. Farrow, M. W. George, M. Kogimtzis, P. Matousek, A. W. Parker, M. R. Pollard, D. A. Robinson, Z. J. Xin and M. Towrie, *Appl. Spectrosc.*, 2010, **64**, 1311–1319; (*b*) G. M. Greetham, D. Sole, I. P. Clark, A. W. Parker, M. R. Pollard and M. Towrie, *Rev. Sci. Instrum.*, 2012, **83**, 103107.

16 A. W. Parker, C. Y. Lin, M. W. George, M. Towrie and M. K. Kuimova, *J. Phys. Chem. B*, 2010, **114**, 3660–3667.

17 N. O. Reich and K. R. Sweetman, *Nucleic Acids Res.*, 1994, **22**, 2089–2093.

18 B. Wellenzohn, W. Flader, R. H. Winger, A. Hallbrucker, E. Mayerm and K. R. Liedl, *Nucleic Acids Res.*, 2001, **29**, 5036–5043.

19 P. Lincoln and B. Nordén, *J. Phys. Chem. B*, 1998, **102**, 9583–9594.

20 (*a*) Q. Cao, C. M. Creely, T. S. Easun, J. Dyer, T. L. Easun, D. C. Grills, D. A. McGovern, J. McMaster, J. Pitchford, J. A. Smith, X.-Z. Sun, J. M. Kelly and M. W. George, *Photochem. Photobiol. Sci.*, 2011, **10**, 1355–1364; (*b*) E. D. Olmon, P. A. Sontz, A. M. Blanco-Rodríguez, M. Towrie, I. P. Clark, A. Vlček and J. K. Barton, *J. Am. Chem. Soc.*, 2011, **133**, 13718–13730.

21 L. Wang and T. A. Keiderling, *Nucleic Acids Res.*, 1993, **21**, 4127–4132.

22 (*a*) T. Véry, D. Ambrosek, M. Otsuka, C. Gourlaouen, X. Assfeld, A. Monari and C. Daniel, *Chem.–Eur. J.*, 2014, **20**, 12901–12909; (*b*) C. Daniel, *Coord. Chem. Rev.*, 2015, **282**, 19–32.

23 G. D. Reid, D. J. Whittaker, M. A. Day, D. A. Turton, V. Kayser, J. M. Kelly and G. S. Beddard, *J. Am. Chem. Soc.*, 2002, **124**, 5518–5527.

24 S. J. Devereux, P. M. Keane, S. Vasudevan, I. V. Sazanovich, M. Towrie, Q. Cao, X.-Z. Sun, M. W. George, C. J. Cardin, N. A. P. Kane-Maguire, J. M. Kelly and S. J. Quinn, *Dalton Trans.*, 2014, **43**, 17606–17609.